CHEMISTRY OF MATERIALS

Article

pubs.acs.org/cm

Colloidal Photonic Crystals toward Structural Color Palettes for Security Materials

Hye Soo Lee,[†,‡] Tae Soup Shim,[†,‡] Hyerim Hwang,[†,‡,§] Seung-Man Yang,*[,†,‡] and Shin-Hyun Kim*[,†]

[†]Department of Chemical and Biomolecular Engineering, KAIST, Daejeon, 305-701 Korea

[‡]National Creative Research Initiative Center for Integrated Optofluidic Systems, KAIST, Daejeon, 305-701 Korea

Supporting Information

ABSTRACT: Self-assembly of monodisperse colloidal particles into regular lattices has provided relatively simple and economical methods to prepare photonic crystals. The photonic stop band of colloidal crystals appears as opalescent structural colors, which are potentially useful for display devices, colorimetric sensors, and optical filters. However, colloidal crystals have low durability, and an undesired scattering of light makes the structures white and translucent. Moreover, micropatterning of colloidal crystals usually requires complex molding procedures, thereby limiting their practical applications. To overcome such shortcomings, we develop a pragmatic and amenable method to prepare colloidal photonic crystals with high optical transparency and physical rigidity using photocurable colloidal suspensions. The colloidal particles dispersed in a photocurable medium crystallized during capillary force-induced infiltration into a slab, and subsequent photopolymerization of the medium permanently solidifies the structures. Furthermore, conventional photolithography enables micropatterning of the crystal structures. The low index contrast between particles and matrix results in high transparency of the resultant composite structures and narrow reflection peaks, thereby enabling structural color mixing through the overlapping of distinct layers of the colloidal crystals. Multiple narrow peaks in the spectrum provide high selectivity in optical identification, thereby being potentially useful for security materials.

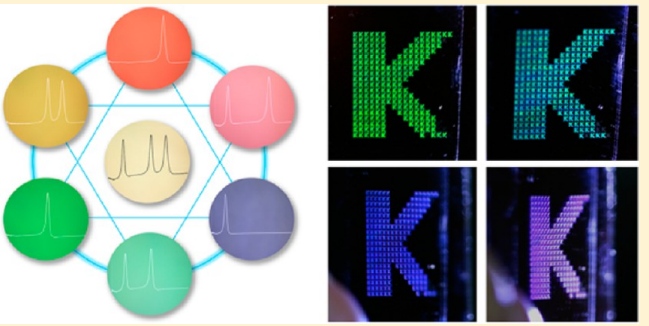

KEYWORDS: *colloids, colloidal crystals, photonic crystals, structural color, lithography*

1. INTRODUCTION

Colloidal crystals have long been studied, owing to their unique optical properties and their applications as photonic crystals.[1−4] The periodic modulation of the refractive index in regular arrays of colloidal particles gives rise to photonic bandgap properties. Light with energy in the bandgap cannot propagate through such materials, resulting in reflection of the light.[5−7] Colloidal crystals with a periodicity on the scale of half the wavelength of visible light exhibit a stop band that manifests as structural colors, similar to natural opals.[3] A variety of photonic and optical applications have been demonstrated based on the stop band and structural color. For example, patterning the colloidal crystals or dynamically tuning the periodicity could potentially be used as a basis for color displays in the reflection mode,[8−12] and the insertion of active defects into colloidal crystals or doping such crystals with light emitters enables the creation of optical waveguides[13] and lasers,[14−16] respectively. Structural colors have also been used in colorimetric chemical sensors and iridescent pigments.[17,18] Such colors are also potentially useful for anticounterfeiting materials,[19] as simple copying cannot duplicate structural colors. To achieve such applications, various techniques for colloidal crystallization have been developed, including evaporation- or shear-induced self-assembly[20,21] and interparticle repulsion-induced crystallization.[17] However, several challenges remain. Most colloidal crystals are difficult to prepare in freestanding films or micropatterns due to the complicated fabrication procedures required and the fragility of the structures formed. These drawbacks severely limit the practical utility of such structures. Furthermore, colloidal crystals are opaque due to strong scattering, making the mixing of structural colors from multilayer structures difficult. Therefore, the development of a practical platform to produce transparent and tailorable colloidal photonic crystals remains an important but unmet need.

Here, we report a facile and practical method for the creation of highly transparent colloidal photonic crystal films using photocurable colloidal suspensions. The colloidal particles dispersed in a photocurable resin formed face-centered cubic (fcc) lattices through shear-induced crystallization of repulsive colloids, and UV-induced photopolymerization enabled the rapid solidification and micropatterning of the crystal structure through photolithography. Of particular interest in this context is that the high transparency of the composite film enabled the

Received: April 18, 2013
Revised: June 6, 2013

 © XXXX American Chemical Society dx.doi.org/10.1021/cm4012603 | *Chem. Mater.* XXXX, XXX, XXX−XXX

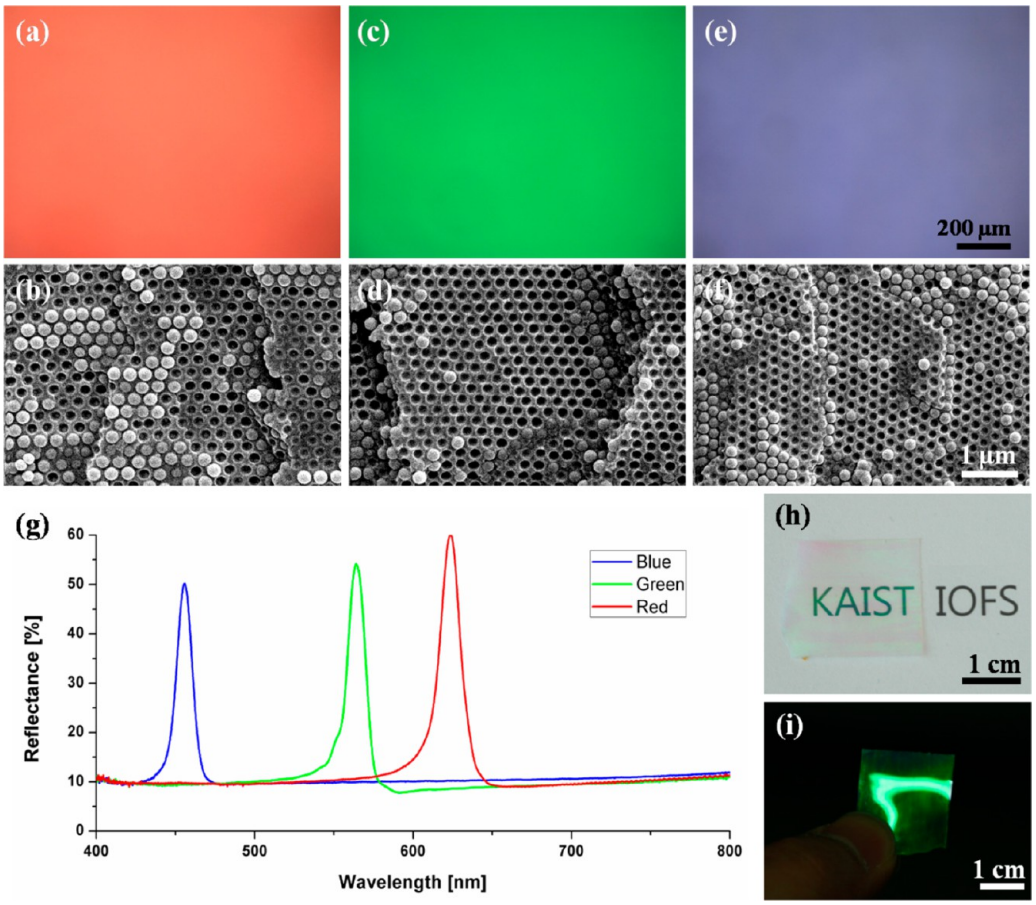

Figure 1. (a–f) Three sets of optical microscopy images of silica-ETPTA composite films and scanning electron microscopy (SEM) images showing their cross sections, where the three films are composed of silica particles 200 nm (a, b), 178 nm (c, d), and 146 nm (e, f) in diameter at a volume fraction of 0.33. (g) Reflectance spectra of the three composite films shown in a–f. (h, i) Images of the composite film showing high transparency under ambient light (h) and bright reflection colors under conditions where the angle of incidence is the same as the reflection angle (i).

formation of multiple reflection peaks, via the overlapping of distinct layers of the colloidal crystals, with no deterioration in the optical properties. In addition, the low index contrast induced narrow stop bands and therefore narrow peaks in the spectrum, providing high selectivity for various optical applications such as optical identification and optical filtering. Although multilayers of colloidal crystals formed from different particle sizes have been prepared using sequential vertical depositions,[22,23] in these investigations either the optical properties were not evaluated or they were poor due to low optical transmission caused by undesired scattering in the colloidal structures with high refractive index contrast.

2. EXPERIMENTAL SECTION

Preparation of the Suspensions. Silica particles with various sizes were prepared using a combination of the two-phase method for the synthesis of seed nanoparticles and the Stöber method for the growth of the nanoparticles to submicrometer size; polydispersity was typically 0.025.[24] The silica particles were washed with ethanol several times and then dried to measure the weight. The silica powders were redispersed in about 2 mL of ethanol, and the ethanolic suspensions were mixed with ethoxylated trimethylolpropane triacrylate (ETPTA, Aldrich) containing 1 wt % Darocur 1173 or 0.5 wt % Irgacure 2100 (Ciba Specialty Chemicals) as a photoinitiator, where the amounts of ETPTA were determined to set the volume fraction of silica as 0.33 in the ethanol-free base; for example, 1 mL of ETPTA solution was added into the ethanol suspension of 1 g of silica particles. The ethanol was then selectively evaporated from the mixture by heating at 70 °C for 12 h in a convection oven.

Film Casting of Suspensions and Photolithography. To prepare transparent composite films, we employed two parallel glass slides separated by polyimide tape (Kapton, 50 μm in thickness). After infiltration of the silica-ETPTA suspension into the gap under capillary forces, the glass was exposed to UV light from a Ag arc lamp (Inocure 100N, Lichtzen Co., Ltd.) for 1 s. The polymerized films were detached from the glasses carefully and washed with ethanol. To create bilayer films, we infiltrated the second suspension into the gap between the precoated glass slide and a new glass slide, which were separated by 100 μm (two layers of polyimide tape), and then polymerized the suspension. As an alternative approach for sequential film casting, we prepared trilayer films by stacking three single films that were prepared independently, where the gaps between the films were infiltrated with particle-free ETPTA. To make photonic crystal micropatterns, we used an amorphous silicon photomask as one of the two parallel plates; the photomask was prepared using reactive ion etching of the amorphous silicon deposited on the glass wafer, where an AZ5214 (Clariant) micropattern was preformed using photolithography and was used as an etching mask.[25] After infiltrating the silica-ETPTA suspension into the gap between the photomask and the glass slide, we illuminated the suspension with UV light (14.5 mW/cm^2) through the photomask for 3 s, where the photomask was treated with oxygen plasma for 3 min, and the glass slide was treated with 2-[methoxy (polyethyleneoxy)propyl] trimethoxy silane (Gelest, Inc.) for 10 min prior to use. These surface treatments allowed higher adhesion of the resultant structures on the photomask. After detaching the glass slide from the photomask, the unpolymerized suspension was washed away using ethanol. To make freestanding films containing the

dx.doi.org/10.1021/cm4012603 | Chem. Mater. XXXX, XXX, XXX–XXX

micropatterns, particle-free ETPTA was infiltrated into the gap that had a separation of 100 μm and was polymerized via UV exposure without a photomask. To make flexible films containing the micropatterns, a 1:5 (v/v) mixture of propoxylated glycerol triacrylate (OTA480, Cytec Industries, Inc.) and amine-modified polyester acrylate (EB81, Cytec Industries, Inc.) was used instead of ETPTA. To add a new color layer, the silica-ETPTA suspension was infiltrated and polymerized using UV exposure, with or without the film photomask. Porous photonic crystals were prepared via the dissolution of silica particles from the composite films. This was achieved via treatment with a 5% HF solution (50%, Sigma-Aldrich) for 12 h; this is enough time to completely remove all silica particles embedded in 200-μm-thick film

Characterization. The colloidal photonic crystals were observed using an optical microscope in reflection mode (Nikon, L150) with a color digital camera (Nikon, DS-5M), and scanning electron microscope (SEM, Philips, XL30), after Au coating. For the reflectance measurements, we used a spectrometer (OceanOptics Inc., USB4000) mounted on the optical microscope. Transmission spectra were measured using an optical setup containing a monochromator (Spectral Products, DK240) and a Si photo detector (New Focus, Visible Femtowatt Photoreceiver); a fiber-coupled tungsten-halogen lamp (Spectral Products, ASBN-W-020) was used as a light source.

3. RESULTS AND DISCUSSION

3.1. Composite Photonic Films with High Transparency. To fabricate regular arrays of colloidal particles with high transparency, we employed a photocurable resin of ETPTA (n_{ETPTA} = 1.4689) as a dispersion medium for silica particles (n_{silica} = 1.45). Silica particles in ETPTA can form colloidal crystals at volume fractions as low as 15% with the assistance of shearing, due to the repulsive interparticle potential.[9,16,26] This repulsive force results from the disjoining pressure of the solvation layer on the particle surface as well as weak electrostatic repulsion, while weak van der Waals attractions are also present due to the low refractive index contrast.[26,27] When the silica-ETPTA suspension was infiltrated into the space between two parallel glass substrates, the suspension exhibited a uniform reflection color from the surface due to formation of aligned crystals. Then, UV irradiation of the suspension caused it to solidify within 1 s. The position of the stop band could be controlled by changing the particle diameter, D, and volume fraction, ϕ. Because the particles formed fcc lattices with (111) planes aligned along the wide glass surfaces, and each particle maintained equal distances from its 12 nearest neighbors because of interparticle repulsions, we could estimate the wavelength λ of the stop band in the [111] direction (L-gap) using Bragg's law:

$$\lambda = 2dn_{\text{eff}} = \left(\frac{\pi}{3\sqrt{2}\phi}\right)^{1/3}\left(\frac{8}{3}\right)^{1/2} D(n_{\text{silica}}{}^2\phi + n_{\text{ETPTA}}{}^2(1-\phi))^{1/2} \quad (1)$$

where d is the (111) plane spacing and n_{eff} is the effective refractive index of the composite. Three different composite films, composed of silica particles with diameters of D = 200 nm, 178 nm, and 146 nm at ϕ = 0.33, exhibited red (R), green (G), and blue (B) reflection colors, respectively, under light that was normally incident on the surface; Figure 1a–f show three sets of optical microscopy images of the film surface and SEM images of the film cross-section. It is clear from the optical microscopy and SEM images that the larger particles (thus with larger lattice constants) resulted in reflection at longer wavelengths. The colloidal crystals spanned the overall thickness of the film, as shown in the cross-sectional SEM images in Figure S1 in Supporting Information. During the shear-induced crystallization, the particles are crystallized at the surface, and the crystals grow toward the center. In the SEM image, no boundary between two crystals grown from the opposite surfaces is observed, thereby forming large crystals in overall thickness. The particles are all embedded in a polymer matrix even at the surface of the film; this makes the estimation of grain size difficult in the lateral dimension. The reflection spectra for these three composite films showed peaks at 623.8 nm (R), 564.2 nm (G), and 455.8 nm (B), respectively, with small full width at half-maximum (fwhm) values of 14.7 nm, 12.4 nm, and 11.3 nm (see Figure 1g). The ratio of the fwhm to the peak position wavelength, $\Delta\lambda/\lambda$, is roughly proportional to the ratio of the refractive index contrast to the effective refractive index, $\Delta n/n_{\text{eff}}$.[14] The spectra for the R, G, and B films showed $\Delta\lambda/\lambda$ values of 0.0236, 0.0220, and 0.0248, respectively, which were self-consistent, owing to a constant $\Delta n/n_{\text{eff}}$ value of 0.01292. The composite films exhibited significant reflectivity of above 50% at the stop band position and high transparency at wavelengths outside the stop band; in spite of a very small contrast of the reflective index, high reflectivity can be achieved owing to numerous layers of colloidal crystals in the thick film. For example, we could clearly read the word "KAIST" under ambient light when it was covered by the composite film; a typical transmission spectrum for the composite film showed 95% transmittance for wavelengths longer than the stop band wavelengths and 80% transmittance for shorter wavelengths, as shown in Figure S2a. In general, a light with a shorter wavelength has lower transmittance when it propagates through a heterogeneous medium. Reflection of a light with a narrow band of 10–15 nm does not significantly influence overall film transparency. However, the black letters appear weak green; we attribute this to absorbance of the transmitted light of all wavelengths by the black pigment, thereby enhancing the contrast of very weak reflection color under ambient light conditions. The same film showed bright reflection colors when the beam's angle of incidence onto the surface of the composite film coincided with the angle of observation, as shown in Figure 1i, where a short exposure time was used to prevent saturation in the bright region, creating a dark environment around the film. Although the film shows uniform color through all surfaces as shown in Figure S2b, bending of the film produces bright reflection only at local area where the angles of incidence and reflection were the same.

3.2. Multilayered Photonic Films. The high transparency of the composite film enabled the creation of multilayers of photonic crystal films with no deterioration of the optical spectrum from each layer. Through infiltration and subsequent photopolymerization of the silica-ETPTA suspension on a preformed composite layer, we could prepare bilayer films, each of which has a thickness of 50 μm, as shown in Figure 2a–c. The colors in the optical microscopy images appeared as cyan (C), yellow (Y), and magenta (M), which were secondary colors produced by the mixing of two primary colors; the films with C, Y, and M colors were composed of two distinct layers of photonic crystals with colors of B plus G, G plus R, and R plus B, respectively. Photograph of the typical bilayer film is shown in Figure S2c. The reflectance spectra from these three different bilayer films had two distinct peaks, as shown in Figure 2d; the cross-section of the bilayer film with a thickness of 100 μm is shown in the inset. Trilayer films with all of the R,

dx.doi.org/10.1021/cm4012603 | Chem. Mater. XXXX, XXX, XXX–XXX

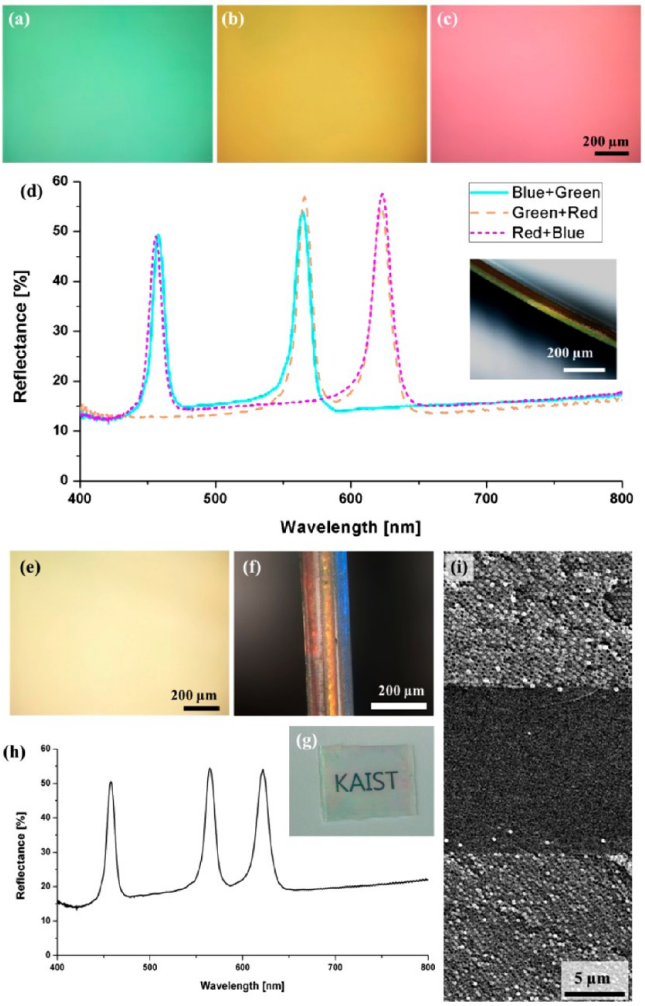

Figure 2. (a–c) Optical microscopy images of the three composite bilayers composed of blue plus green, green plus red, and red plus blue films, at normal reflection. (d) Reflectance spectra of the three films shown in a–c, each of which shows two distinctive narrow peaks. The inset shows the cross-section of the bilayered film shown in b. (e, f) Optical microscopy images showing composite trilayers composed of red, green, and blue films (e) and their cross sections (f). (g) Images of the composite film showing high transparency under ambient light. (h) Reflectance spectrum of the films shown in e–g, showing three distinctive narrow peaks. (i) SEM image showing the two boundaries between the composite and particle-free layers.

G, and B colors could also be prepared by infiltrating particle-free ETPTA between two of the layers after the independent preparation of each layer. The resultant trilayer film displayed as white under an optical microscope, as shown in Figure 2e; the cross-section of the film (which had a thickness of 180 μm) is shown in Figure 2f. The film was still transparent, as shown in Figure 2g. The reflectance spectrum of the trilayer film showed three distinct peaks, as shown in Figure 2h. It is noteworthy that there was almost no reduction in the reflectivity and negligible peak widening. The boundary between the two layers is shown in the SEM image in Figure 2i, where the polymerized particle-free ETPTA was sandwiched by the two layers composed of silica particles, which had D values of 146 and 180 nm, respectively. On the basis of these multistacks, we could potentially produce a palette of structural colors by controlling the relative reflectivity of the composite photonic crystals with three primary colors; the reflectivity can be controlled by changing the thickness of the film. In addition, the narrow peaks in the spectra were highly wavelength-selective, and multiple peaks further enhanced the selectivity, providing an abundance of distinguishable, easily identified optical signals or codes. Such multistacks of composite layers could therefore be useful for security materials or spectrometric encoding.

3.3. Micrpatterned Photonic Films. The photocurable suspension could be patterned using photolithography, producing micropatterning of the colloidal photonic crystals. To demonstrate this, we infiltrated a silica-ETPTA suspension with D = 180 nm and ϕ = 0.33 into the gap between a glass slide and an amorphous silicon photomask separated by 50 μm, as illustrated in the first schematic shown in Figure 3a.[25] The photomask pattern, comprised of arrays of small K windows, was transferred into the composite photonic crystals during UV illumination through the photomask, and the subsequent washing of unpolymerized suspension with ethanol left behind an array of small K's on the photomask, as shown in the second schematic in Figure 3a. Each of the small K colloidal crystals exhibited the bright reflection of green light under normally incident light; the reflection color blue-shifted as the angle of incident light increased from 10° to 55°, as shown in Figure 3b. The array could be transferred into a freestanding film by forming a particle-free ETPTA film in the interstices between small K's as shown in the third and fourth schematics in Figure 3a and the optical image in Figure 3c. The resultant film was highly transparent. When we placed the film on a Korean bank note, it was difficult to discern the film (bottom right image in Figure 3d). When the angle of incidence of the light was the same as the angle of reflection, however, the film exhibited a bright reflection color, as shown in the main image in Figure 3d; for higher incident and reflection angles, the color was blue-shifted (top right image in Figure 3d). This photonic crystal pattern is therefore promising for security materials for anticounterfeiting or optical identification codes. The film can be flexible and foldable by employing monomers which produce a rubber-like polymer, as shown in Figure S3.

The small K's could be released from the photomask by mechanically swiping a blade along the surface, forming particles suspended in liquid; particles suspended in ethanol are shown in Figure S4, where the particles that satisfied the reflection condition—i.e., the angles of incidence and reflection were the same—exhibited a green color, while the others appeared as transparent. In the same fashion, microdisk particles of diameter 200 μm could be prepared using photolithography. We used these particles as color pigments for decorative painting after selective dissolution of the silica particles from the polymerized ETPTA matrix. This dissolution of the silica particles resulted in a more vivid and blue-shifted color, due to the higher index contrast and the decrease in the effective index. The porous particles were dispersed in an acetone solution of nitrocellulose (the ingredients in nail varnish) and were used to coat a glass surface, as shown in Figure S5. The coated microdisks displayed strong green colors under normally incident light, and the color was blue-shifted as the angle of incidence of the light increased. The feature size of the photonic disks can be further reduced up to the thickness of the film, 50 μm for this case.

3.4. Multicolored Micropatterns. The small-K patterns could be further colorized and patterned via a second photolithography step, as shown in Figure 4a. Instead of particle-free ETPTA, a silica-ETPTA suspension with D = 205

dx.doi.org/10.1021/cm4012603 | Chem. Mater. XXXX, XXX, XXX–XXX

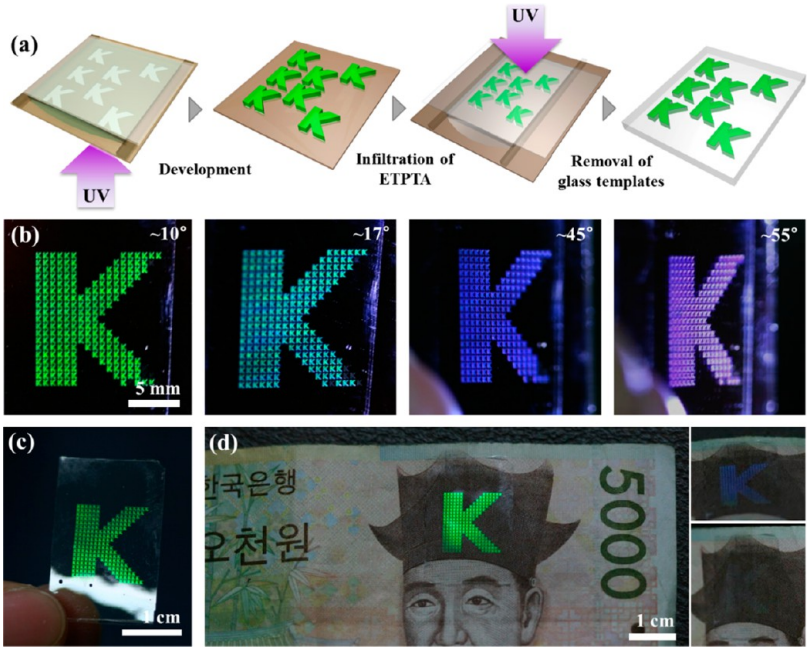

Figure 3. (a) Schematic illustration of the method used to make colloidal crystal patterns or freestanding films containing the patterns. Photolithography with an amorphous silicon photomask on a glass wafer enables the patterning of small K's, and subsequent infiltration and polymerization of particle-free ETPTA enables the preparation of a freestanding film with a photonic crystal pattern. (b) Optical images of the colloidal crystal pattern composed of small K's that show a reflection color that strongly depends on the angle of incidence of the light, which is given in each image. (c) Optical image of a freestanding film containing a pattern of small K's. (d) The patterned photonic crystal film on a Korean bank note; the pattern exhibits bright green color under normal reflection (main image), while the pattern displays a blue color for high incident and reflection angles (top right). The film is highly transparent and difficult to distinguish when the viewing angle is different from the angle of incidence of the light (bottom left).

nm and ϕ = 0.33 was infiltrated into the gap between a glass slide and an amorphous silicon photomask (separated by 100 μm) and was then illuminated with UV light through an additional photomask mounted on top of the glass slide, as shown in the first and second schematics in Figure 4a; the additional photomask had a large K window that covered all of the small K's on the surface of the amorphous silicon. After the development of the unpolymerized suspension, we obtained a large, red-colored K that contained small, greenish K's, as shown in the third schematic in Figure 4a and the optical image in Figure 4b. This dual-colored pattern formed a freestanding film after it was detached from the bottom substrate, as shown in Figure S6. To add a third color, we infiltrated a silica-ETPTA suspension with D = 155 nm and ϕ = 0.33 into the gap between the parallel glass slide and the amorphous silicon photomask (separated by 150 μm) and illuminated the sample with UV light. The resultant pattern contained small, greenish K's along with large, reddish K's, set against a bluish background (Figure 4c). All of the colors were blue-shifted for non-normally incident light (Figure 4d). The pattern was also freestanding and transparent after detachment from the amorphous silicon photomask (Figure S7). The reflectance spectrum varied depending on the location on the film, as shown in Figure 4e; this figure includes optical microscopy images taken at the locations where the reflectance spectra were measured. Because the small K's were composed of three layers of G, R, and B, all with a thickness of 50 μm, they exhibited three distinct peaks and a whitish appearance in the optical microscopy image. Unlike this whitish appearance under an optical microscope with normal incident and reflection beams to the surface of the film, a macroscopic photograph of the film shows a greenish appearance from the top layer, as shown in Figure 4c; we attribute this to deviation of the incident and reflection angles from 0° and the existence of ambient light. In contrast, the large K's—which were composed of two layers of R with a thickness of 100 μm, and a B layer with a thickness of 50 μm—exhibited two peaks, and a magenta color in the optical microscopy image. The background, which was composed of one thick layer with a thickness of 150 μm, showed one peak and a blue color in the optical microscopy image. A typical transmission spectrum of the trilayered film is shown in Figure S7c.

3.5. Porous Photonic Films. To compare the optical characteristics of photonic crystals with high index contrast, we prepared porous photonic crystal films via the selective dissolution of silica particles from a bilayer composite film composed of R and G layers. Because the silica particles were replaced by air cavities, the refractive index contrast increased from 0.0689 to 0.4689, and the effective index decreased from 1.4465 to 1.3325, resulting in increases in the bandwidth and a blue-shift in the bandgap position, respectively. Optical microscopy images of the porous film taken from two different sides, and the corresponding reflectance spectra, are shown in Figure 5; the peaks in the blue and green curves had FWHMs of 41.6 and 46.3 nm centered at wavelengths of 486.8 and 562.2 nm, respectively. The $\Delta\lambda/\lambda$ values were therefore 0.0855 and 0.0824, which was consistent with the large $\Delta n/n_{\mathrm{eff}}$ value of ~0.352. In addition, the large index contrast induced a high reflectivity of approximately 80%. The cross-section of the porous bilayer film is shown in the inset of Figure 5c, where the boundary between the two layers is illustrated with a white dotted line. Unlike the transparent composite film, the porous film was almost opaque, due to strong scattering in the structure (which had a large index contrast). Therefore, only

dx.doi.org/10.1021/cm4012603 | Chem. Mater. XXXX, XXX, XXX–XXX

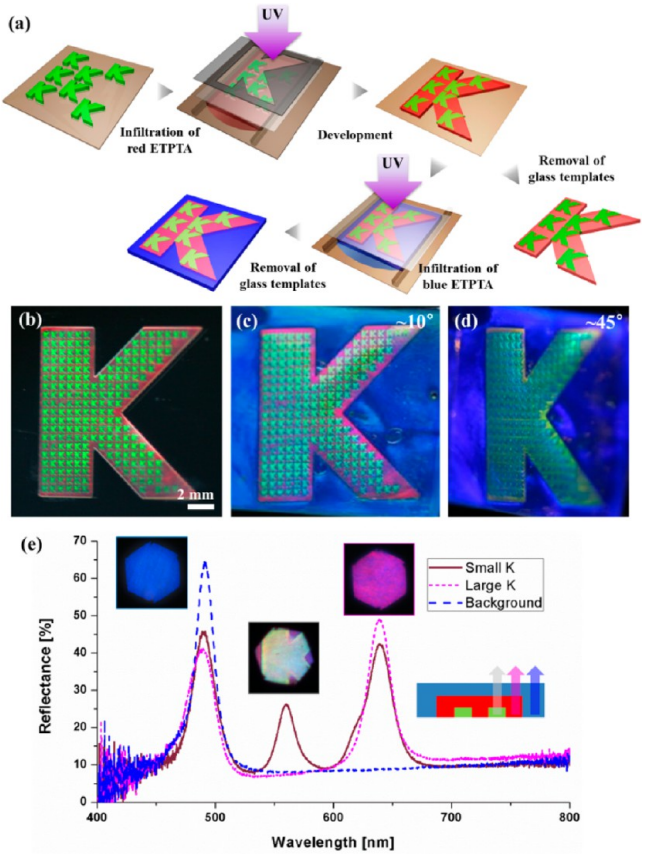

Figure 4. (a) Schematic illustration of the method used to make colloidal crystal patterns with two or three distinct colors. The second photolithography process using a photomask with a large K window mounted on cover glass enables the patterning of a large K on the pre-existing small-K pattern. The large K can be formed as a freestanding film by releasing it from the substrate. Alternatively, the background of the large K can be created as a blue-colored film through an additional step involving the infiltration and polymerization of an ETPTA suspension. (b–d) Optical images of the freestanding film with two colors (b) and three colors (c, d); the small K, large K, and background exhibit green, red, and blue colors, respectively, under normal reflection. (e) Reflectance spectra and optical microscopy images of the freestanding film taken in local areas on the small K, large K, and background.

the top layer influenced the reflection spectrum and color. The reflectance spectrum taken from the green layer side had only one main peak, and the spectrum from the blue layer side showed a very small peak at the green wavelength, owing to the low transmittance.

4. CONCLUSION

We have demonstrated a practical method to create highly transparent colloidal photonic crystals and multilayer structures created from these materials using photocurable suspensions. The low index contrast between the colloidal silica particles and the photocurable resin facilitated shear-induced crystallization and gave rise to high transmission while maintaining high reflectivity in the stop band, thereby enabling the formation of multiple peaks in the reflectance spectra from the multilayered photonic crystals. The combination of the primary structural colors of R, G, and B resulted in secondary colors of C, M, and Y, as well as white. In addition, the various combinations of these primary colors with controlled relative reflectivity could

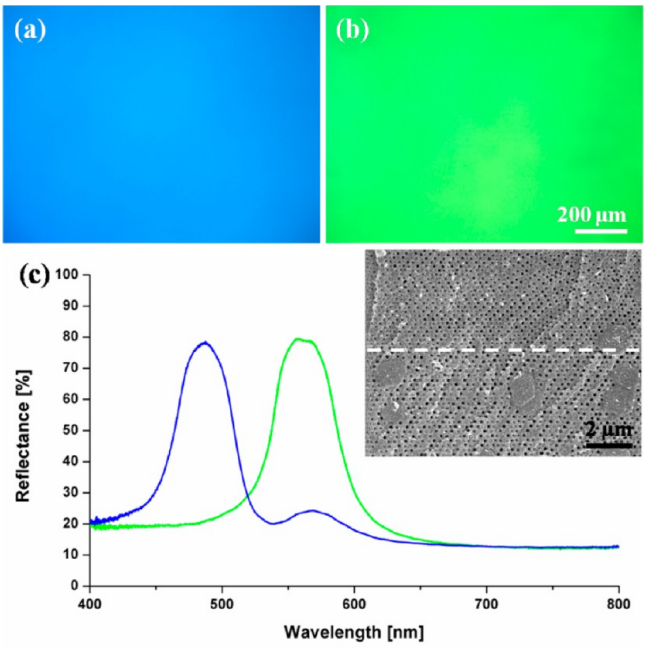

Figure 5. (a, b) Optical microscope images of porous bilayers composed of green and blue films where a and b were taken from the blue and green layer sides, respectively. (c) Reflectance spectra of the porous bilayers taken from blue (blue line) and green layer sides (green line). The inset is the SEM image showing the interface between two layers.

potentially provide a full optical palette of structural colors, or an abundance of available spectrometric codes. Moreover, such structural colors can be patterned easily using simple photolithography. Multiple photolithography steps produced multicolored photonic crystal micropatterns. We demonstrated two different applications of our transparent photonic crystals. When coated on important documents or paper money, the photonic crystal patterns can provide optical codes and prevent counterfeiting, and small photonic particles can be used as iridescent structural color pigments for cosmetics, paints, and decorative coatings. In addition, the multiple peaks in the reflectance will be useful in a wide range of photonic applications, including optical filters and reflectors.

■ ASSOCIATED CONTENT

Ⓢ Supporting Information

Additional experimental results discussed in the text (Figures S1–S7; PDF). This material is available free of charge via the Internet at http://pubs.acs.org.

■ AUTHOR INFORMATION

Corresponding Author

*E-mail: kim.sh@kaist.ac.kr (S.-H.K.); smyang@kaist.ac.kr (S.-M.Y.).

Present Address

[§]Harvard School of Engineering and Applied Sciences, Cambridge, MA 02138 U. S. A.

Notes

The authors declare no competing financial interest.

■ ACKNOWLEDGMENTS

This work was supported by a grant from the Creative Research Initiative Program of the Ministry of Education, Science and

Technology for "Complementary Hybridization of Optical and Fluidic Devices for Integrated Optofluidic Systems".

REFERENCES

(1) Xia, Y.; Gates, B.; Yin, Y.; Lu, Y. *Adv. Mater.* **2000**, *12*, 693.
(2) Lopez, C. *Adv. Mater.* **2003**, *15*, 1679.
(3) Marlow, F.; Muldarisnur; Sharifi, P.; Brinkmann, R.; Mendive, C. *Angew. Chem., Int. Ed.* **2009**, *48*, 6212.
(4) Kim, S.-H.; Lee, S. Y.; Yang, S.-M.; Yi, G.-R. *NPG Asia Mater.* **2011**, *3*, 25.
(5) Yablonovitch, E. *Phys. Rev. Lett.* **1987**, *58*, 2059.
(6) Tarhan, I. I.; Watson, G. H. *Phys. Rev. Lett.* **1996**, *76*, 315.
(7) Xia, Y.; Gates, B.; Li, Z.-Y. *Adv. Mater.* **2001**, *13*, 409.
(8) Kim, H.; Ge, J.; Kim, J.; Choi, S.-E.; Lee, H.; Lee, H.; Park, W.; Yin, Y.; Kwon, S. *Nat. Photonics* **2009**, *3*, 534.
(9) Kim, S.-H.; Park, H. S.; Choi, J. H.; Shim, J. W.; Yang, S.-M. *Adv. Mater.* **2010**, *22*, 946.
(10) (a) Arsenault, A. C.; Puzzo, D. P.; Manners, I.; Ozin, G. A. *Nat. Photonics* **2007**, *1*, 468. (b) Puzzo, D. P.; Arsenault, A. C.; Manners, I.; Ozin, G. A. *Angew. Chem., Int. Ed.* **2009**, *48*, 943.
(11) Shim, T. S.; Kim, S.-H.; Sim, J. Y.; Lim, J.-M.; Yang, S.-M. *Adv. Mater.* **2010**, *22*, 4494.
(12) Arsenault, A.; Fleischhaker, F.; von Freymann, G.; Kitaev, V.; Miguez, H.; Mihi, A.; Tetreault, N.; Vekris, E.; Manners, I.; Aitchison, S.; Perovic, D.; Ozin, G. A. *Adv. Mater.* **2006**, *18*, 2779.
(13) Rinne, S. A.; García-Santamaría, F.; Braun, P. V. *Nat. Photonics* **2008**, *2*, 52.
(14) Shkunov, M. N.; Vardeny, Z. V.; DeLong, M. C.; Polson, R. C.; Zakhidov, A. A.; Baughman, R. H. *Adv. Funct. Mater.* **2002**, *12*, 21.
(15) Lawrence, J. R.; Shim, G. H.; Jiang, P.; Han, M. G.; Ying, Y.; Foulger, S. H. *Adv. Mater.* **2005**, *17*, 2344.
(16) Kim, S.-H.; Kim, S.-H.; Jeong, W. C.; Yang, S.-M. *Chem. Mater.* **2009**, *21*, 4993.
(17) (a) Asher, S. A.; Holtz, J.; Liu, L.; Wu, Z. *J. Am. Chem. Soc.* **1994**, *116*, 4997. (b) Holtz, J.; Asher, S. A. *Nature* **1997**, *389*, 829.
(18) (a) Kim, S.-H.; Lee, S. Y.; Yi, G.-R.; Pine, D. J.; Yang, S.-M. *J. Am. Chem. Soc.* **2006**, *128*, 10897. (b) Zhao, Y. J.; Zhao, X. W.; Sun, C.; Li, J.; Zhu, R.; Gu, Z. Z. *Anal. Chem.* **2008**, *80*, 1598.
(19) Hu, H.; Chen, Q.-W.; Tang, J.; Hu, X.-Y.; Zhou, X.-H. *J. Mater. Chem.* **2012**, *22*, 11048.
(20) (a) Jiang, P.; Bertone, J. F.; Hwang, K. S.; Colvin, V. L. *Chem. Mater.* **1999**, *11*, 2132. (b) Wong, S.; Kitaev, V.; Ozin, G. A. *J. Am. Chem. Soc.* **2003**, *125*, 15589.
(21) Jiang, P.; McFarland, M. J. *J. Am. Chem. Soc.* **2004**, *126*, 13778.
(22) Jiang, P.; Ostojic, G. N.; Narat, R.; Mittleman, D. M.; Colvin, V. L. *Adv. Mater.* **2001**, *13*, 389.
(23) Egen, M.; Voss, R.; Griesebock, B.; Zentel, R. *Chem. Mater.* **2003**, *15*, 3786.
(24) (a) Yokoi, T.; Sakamoto, Y.; Terasaki, O.; Kubota, Y.; Okubo, T.; Tatsumi, T. *J. Am. Chem. Soc.* **2006**, *128*, 13664. (b) Hartlen, K. D.; Athanasopoulos, A. P. T.; Kitaev, V. *Langmuir* **2008**, *24*, 1714.
(25) Shim, T. S.; Kim, S.-H.; Heo, C.-J.; Jeon, H. C.; Yang, S.-M. *Angew. Chem., Int. Ed.* **2012**, *51*, 1420.
(26) Kim, S.-H.; Jeong, W. C.; Hwang, H.; Yang, S.-M. *Angew. Chem., Int. Ed.* **2011**, *50*, 11649.
(27) (a) Raghavan, S. R.; Walls, H. J.; Khan, S. A. *Langmuir* **2000**, *16*, 7920. (b) Ge, J.; Yin, Y. *Adv. Mater.* **2008**, *20*, 3485.